Graph Drawing by Classical Multidimensional Scaling: New Perspectives

Mirza Klimenta and Ulrik Brandes

Department of Computer & Information Science, University of Konstanz
{Mirza.Klimenta,Ulrik.Brandes}@uni-konstanz.de

Abstract. With shortest-path distances as input, classical multidimensional scaling can be regarded as a spectral graph drawing algorithm, and recent approximation techniques make it scale to very large graphs. In comparison with other methods, however, it is considered inflexible and prone to degenerate layouts for some classes of graphs.

We want to challenge this belief by demonstrating that the method can be flexibly adapted to provide focus+context layouts. Moreover, we propose an alternative instantiation that appears to be more suitable for graph drawing and prevents certain degeneracies.

1 Introduction

Multidimensional scaling (MDS) denotes a family of dimensionality reduction techniques that aim at representing given dissimilarities as distances in low-dimensional space. In graph drawing, MDS techniques are usually applied to position vertices according to their graph-theoretic distances, and distance scaling [14] is the recommended choice [5,4].

Classical MDS (CMDS) has only occasionally been recognized as an alternative [26,20,7,4], despite its essentially deterministic results and the availability of simple and highly efficient approximation algorithms [3,29,8]. This may be for the same reasons that spectral methods in general are of limited popularity in graph drawing, namely because of their limited adaptability to application-specific layout requirements, and a tendency to result in excessive occlusion for certain classes of sparse graphs. In fact, the recommended use of CMDS is as a fast and reliable initialization method for distance scaling [4].

By proposing two novel uses of CMDS for graph drawing, we attempt to initiate re-consideration of this conceptually elegant and highly efficient method.

The first one is an adaptation for focus+context, a distortion technique that magnifies a region of interest while maintaining its environment. By adapting the input rather than the drawing, more detail is preserved in the periphery.

The second proposal changes the way in which CMDS itself is used. By increasing the number of output dimensions, we determine coordinates that represent distances more accurately, and then use weighted principal component analysis to project them into two- or three-dimensional space such that local details are favored. While this reduces representation accuracy, it increases graph readability.

W. Didimo and M. Patrignani (Eds.): GD 2012, LNCS 7704, pp. 55–66, 2013.

We start with some background on CMDS for graph drawing in Sect. 2. The adaptation for focus+context is presented in Sect. 3 and a modified graph drawing usage scenario in Sect. 4. We conclude with a brief discussion. All graphs used for illustration are available in the University of Florida Sparse Matrix Collection.[1]

2 Classical Multidimensional Scaling

Multidimensional scaling (MDS) refers to a family of dimensionality reduction techniques. Given a set of objects and a matrix of pairwise dissimilarities between them (often assumed to originate from distances in a high-dimensional space), they yield coordinates in some low-dimensional space such that distances in that space represent the input dissimilarities well. See [9,2] for comprehensive treatments and [10] for a recent review.

Classical MDS (CMDS) [31,15] is the oldest such technique, but still one of the most widely used. In this section we briefly recall the main principles of CMDS and how it is applied to draw graphs. We then detail a degree of freedom that is often overlooked, but will prove pivotal in the remainder of this paper.

2.1 CMDS Principles

Given a set of n objects $\{1,\dots,n\}$ and a matrix $\Delta = (\delta_{ij})$ of pairwise dissimilarities, positions $P \in \mathbb{R}^{n\times d}$ in d-dimensional Euclidean space, $d \ll n$, are sought. Note that by convention we use row vectors for positions $p_i = (p_i^{(1)},\dots,p_i^{(d)})$, $i = 1,\dots,n$.

Classical MDS was proposed independently in [31,15]. It is best understood as a reconstruction approach: assume that the given dissimilarities actually are Euclidean distances arising from object positions $X \in \mathbb{R}^{n\times d'}$ in some d'-dimensional space. Distances are related to inner products of position vectors via

$$\|x_i - x_j\|^2 = (x_i - x_j)(x_i - x_j)^T = x_i x_i^T - 2x_i x_j^T + x_j x_j^T \ ,$$

so that all distances can be computed from entries of the matrix XX^T of inner products. CMDS can be seen as an attempt to reverse this derivation. Given Δ, first construct a matrix of inner products. Unlike distances, however, inner products are not invariant under translation. The standard method to remove this degree of freedom is to translate the configuration such that its centroid is at the origin. We will reconsider this choice in Section 2.3. It can be shown that $B = (b_{ij})_{i,j=1,\dots,n}$ with

$$b_{ij} = -\frac{1}{2}\left(\delta_{ij}^2 - \frac{1}{n}\sum_{r=1}^{n}\delta_{rj}^2 - \frac{1}{n}\sum_{s=1}^{n}\delta_{is}^2 + \frac{1}{n^2}\sum_{r=1}^{n}\sum_{s=1}^{n}\delta_{rs}^2\right)$$

is the matrix of inner products for the translated configuration. The transformation setting row and column means to zero is called *double centering*. Positions

[1] `http://www.cise.ufl.edu/research/sparse/matrices/`

reproducing these inner products are obtained from (partial) *spectral decomposition*,

$$B = U\Lambda[d]U^T = \underbrace{U\Lambda[d]^{1/2}}_{P} \cdot \underbrace{\Lambda[d]^{1/2}U^T}_{P^T}$$

where $\Lambda[d]$ is the diagonal matrix of the d largest eigenvalues of B and $U \in \mathbb{R}^{n\times d}$ is a matrix of corresponding orthonormal eigenvectors. The inner products PP^T are the best d-dimensional reconstruction of B according to the Frobenius norm. In other words, the positions obtained from CMDS minimize

$$strain(B, P) = \|XX^T - PP^T\|_F^2 = \sum_{i=1}^{n}\sum_{j=1}^{n}(b_{ij} - p_i p_j^T)^2 \ . \tag{1}$$

Note that squared errors imply a bias toward the fit of large inner products. CMDS thus generalizes *principal component analysis* (PCA) [33] which indeed requires that X is given.

2.2 CMDS in Graph Drawing

In graph drawing, CMDS is typically applied to shortest-path distances $\delta_{ij} = d_G(i,j)$, $i,j \in V$, of undirected graphs $G = (V,E)$. This yields straight-line drawings in d-dimensional space in which, in general, structurally close vertices are near each other and structurally distant vertices are far apart.

Although determining the distance matrix Δ and decomposing the inner product matrix B is costly in general, very fast approximation algorithms exist [29,3,8,32]. We use PivotMDS [3], which determines distances only from k selected pivot vertices, and therefore runs in time $\mathcal{O}(k(m + kn))$. Since usually $n \gg 100 \geq k \gg d$, approximate CMDS can be used to draw very large graphs.

Although shortest-paths CMDS is generally good at displaying symmetries, the preferred MDS variant for graph drawing is based on weighted fitting of distances directly (rather than via inner products) by minimizing a *stress* function [14], the main reason being better representation of local details [5,4]. Stress minimization, on the other hand, is computationally more involved and sensitive to local minima [4]. It was therefore argued that its bias toward large distances makes CMDS an ideal initialization for *stress* minimization [5,4]. Due to the negligible running time of approximate CMDS, this is a fast and simple alternative to multilevel approaches.

2.3 Choosing an Origin

We have already pointed out that the location of the origin is a degree of freedom in CMDS and most often resolved by double-centering. Unless we are actually reconstructing positions in d-dimensional space from their Euclidean distances, however, this choice has an effect on the resulting layouts. While alternatives have been discussed in various contexts [1,2,16,17], we are not aware of any utilization for graph drawing.

To understand how the origin can be determined before even knowing any positions, assume first that we want the origin to coincide with the position of an object $o \in \{1, \ldots, n\}$. We refer to this object as the *central* object. After positions p_i are obtained from CMDS on dissimilarities δ_{ij}, denote the resulting distances by $d_{ij} = \|p_i - p_j\|$. From the cosine law it follows that

$$d_{ij}^2 = d_{io}^2 + d_{jo}^2 - 2d_{io}d_{jo} \cdot \cos(\alpha)$$

where α is the angle formed by $\overrightarrow{p_o p_i}, \overrightarrow{p_o p_j}$. The inner products can therefore be written as

$$p_i p_j^T = d_{io}d_{jo} \cdot \cos(\alpha) = -\frac{1}{2}(d_{ij}^2 - d_{io}^2 - d_{jo}^2) \ ,$$

in terms of distances only. We therefore set up the inner product matrix B by letting $b_{ij} := -\frac{1}{2}(\delta_{ij}^2 - \delta_{io}^2 - \delta_{jo}^2)$.

This suggests that we can generalize the approach to arbitrary linear combinations of object positions for the origin. In the definition of b_{ij}, we only have to replace the $\delta_{\cdot o}^2$ by corresponding combinations. Note that double-centering thus becomes the special case in which every object is weighted by $\frac{1}{n}$.

Applying CMDS to the distance matrix $\Delta = (\delta_{ij})$ of an undirected graph yields distances $D = (d_{ij})$ for which $d_{ij} \approx \delta_{ij}$ in low-dimensional space. Hence, choosing an origin as a linear combination of vertex positions not only results in a translation, but also affects relative positions. In particular, if the origin is defined by a single vertex, the desired angle α between positions of vertices that are both distant from the central vertex is pronounced. This effect will be formalized in Sect. 4.3.

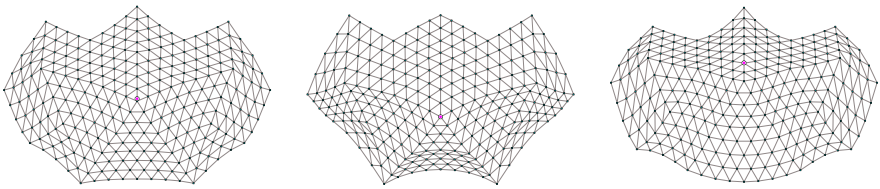

(a) *double centered* (b) *centered on* v_{125} (c) *graph centered*

Fig. 1. Choosing an origin for `lshp265` ($n = 265, m = 1009$)

We illustrate the effect in Figs. 1 and 2, where CMDS with double centering is compared to CMDS with other centers. If the origin is defined by the average of all vertices i with minimum eccentricity $\max_{j \in V} d_G(i, j)$, we say that CMDS is *graph centered*.

3 Focus+Context

Focus+context is an essential interaction technique in information visualization [6]. It facilitates the detailed inspection of a region of interest while maintaining the context of the surrounding.

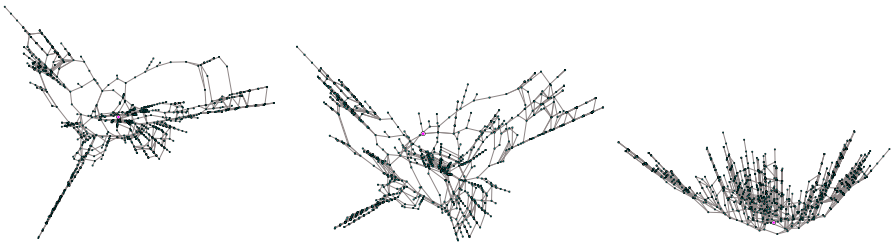

(a) *double centered* (b) *centered on* v_{79} (c) *graph centered*

Fig. 2. Choosing an origin for `1138bus` ($n = 1138$, $m = 2596$)

In addition to focus-dependent relevance filtering, the main principle used in focus+context techniques is distortion. Applications in graph drawing typically distort a given layout (e.g., using a fisheye lense [11]) or the graph itself (e.g., by expanding nodes in a clustered graph [30]) which then requires computation of a new layout.

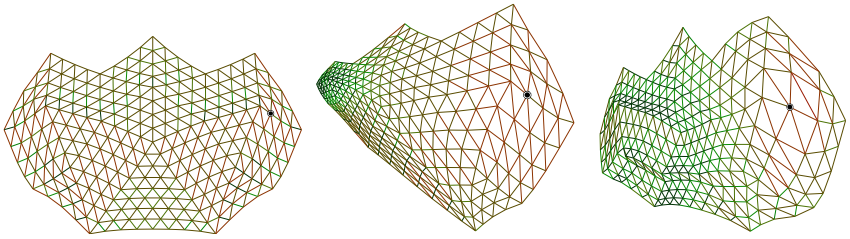

(a) *CMDS layout* (b) *approach from [22]* (c) *our approach*

Fig. 3. Result of *visual emphasis* for `lshp265` ($n = 265, m = 1009$), $o = v_{85}$. The color-scale follows *short* $\rightarrow$ *long* edge lengths

Any given drawing can be distorted using appropriate lenses [28,27]. An example is given in Fig. 3(b), where the layout of Fig. 3(a) is distorted using the method of [22]. We show in this section, however, that CMDS can also be adapted by modifying the input, yielding results as shown in Fig. 3(c). Since drawings are already distorted representations of the input, the more direct control over additional distortions helps in preserving context features.

The idea is to center CMDS on the focal vertex, or vertices, and distort the desired inner products of other vertex positions according to their distance from the focus. It can be shown that distortion of inner products can also be expressed as a distortion of distances, though in less convenient form.

Let $sgn(a) : \mathbb{R} \rightarrow \{-1, 0, 1\}$ be the *signum function*. With $b_{ij}(r, q)$ denoting new inner products, a non-linear modification on b_{ij} follows, $i, j \in V$,

$$b_{ij}(r, q) := sgn(b_{ij}) \cdot (\delta_{io}\delta_{jo})^r \cdot |cos(\alpha)|^q, \tag{2}$$

with $\{r, q\} \in (0, 1)$, hence defining a *concave power function (cpf)*. With the setting $r = q$, the update simplifies to $b_{ij}(r, q) := sgn(b_{ij}) \cdot |b_{ij}|^r$.

The function $sgn(a)$ preserves the orientation of points around the focus. The use of a *cpf* with distances induces gradually diminishing difference in primarily equidistant BFS distances. Given that $\delta^2_{jo} = b_{jj}$, new distances δ'_{jo} to the origin follow $\delta'_{jo} = \delta^r_{jo}$, thereby imposing the focal emphasis. The use of *cpf* with angles, $0 \leq |cos(\alpha)|^q \leq 1$ (also with $q \geq 1$), affects distances δ_{ij}, $i \neq j \in V$.

Figure 4 demonstrates the method results with different foci and parameter choices. Our focus+context approach retains characteristics of the CMDS

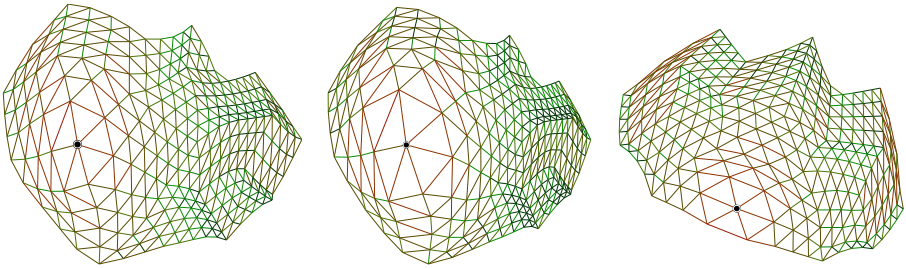

(a) $p_o = p_{84}$, $r = q = 0.6$ (b) $p_o = p_{84}$, $r = q = 0.45$ (c) $p_o = p_{184}$, $r = q = 0.6$

Fig. 4. Focus+context for `lshp265` with focus position p_o

solution centered on a chosen focus. As already shown (see Fig. 2), each origin choice with graphs having intrinsic dimensionality $d > 2$ implies a potentially more dramatic change. Such a change is inherited by the modified layouts, as shown in Fig. 5. The intrinsic dimensionality is studied in Sect. 4.

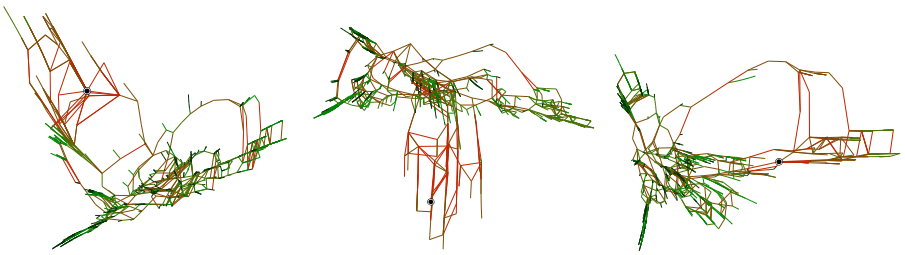

(a) $p_o = p_{241}$ (b) $p_o = p_{568}$ (c) $p_o = p_{723}$

Fig. 5. Focus+context for `1138bus` with focus position p_o; $r = 0.65$, $q = 1$

Multifocal Views. A usual adjustment of focus+context techniques is for *multiple foci* [22,23,13]. Our *input space* manipulation can also be adopted for such a task by interpolating the inner product matrices sharing a common origin. This translation is necessary because the inner products are *translation variant*.

Let $e_i \in \mathbb{R}^n$ be the i^{th} column of the identity matrix $I_n \in \mathbb{R}^{n \times n}$, and let $1_n = [1, \ldots, 1]^T \in \mathbb{R}^n$. Define a *projector* $S_i = (I_n - 1_n e_i^T) \in \mathbb{R}^{n \times n}$, satisfying $S_i S_i = S_i$. It can be shown that a matrix of inner products B^{k_1} centered at p_{k_1} can be translated and centered at p_{k_2} by $B^{k_2} = S_{k_2} \cdot B^{k_1} \cdot S_{k_2}^T$.

Given inner-product matrices $B^{(k_1)}(r_1, q_1), ..., (r_t, q_t)$, $B^{(k_2)}(r_1, q_1), ..., (r_t, q_t)$, $\ldots$, $B^{(k_t)}(r_1, q_1), ..., (r_t, q_t)$ corresponding to t different foci, the interpolation is obtained by

$$B^{(K)} = S_k \left(\sum_{i=1}^{t} \gamma_i \cdot B^{(k_i)} \right) S_k^T, \tag{3}$$

for some $k \in V$, and with γ_i affecting the influence of a particular $B^{(k_i)}$. Note that the setting $S = (I_n - \frac{1}{n} 1_n 1_n^T)$ leads to the *centroid* as the common origin. Fig. 6 illustrates the results. The choice of the common origin affects the result, for the reason discussed previously.

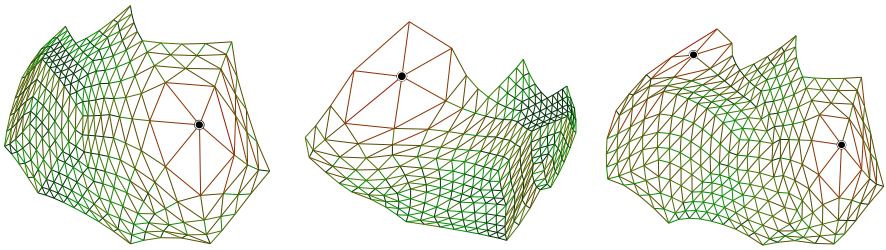

(a) *Focus 1* (b) *Focus 2* (c) *Foci 1, 2* ; $\gamma_1 = \gamma_2 = 1$

Fig. 6. Multifocal view of `lshp265`. $r = 0.45$, $q = 1$; S_{44} used

4 A Better Perspective on a Better Drawing

By design, CMDS is a greedy method: each additional output dimension reduces the representation error by the maximum possible. A layout with maximum representation accuracy in terms of *strain* (1), however, is not necessarily optimal in terms of graph readability because of the greedy matching of large distances. Subsequent dimensions may be responsible for the decisive displacements that make local structures visible. An very graphical example is shown in Fig 7(a).

The main reason why distance scaling is generally preferred for graph drawing is that the *stress* function it attempts to optimize assigns higher weights to small distances. In CMDS, the influence of small distances comes to bear only in dimensions beyond d.

For the closely related PCA (see Sect. 2), weighted approaches have been developed to impose constraints on the projection (e.g., [24,25]). PCA, however, requires that positions are known. To draw a graph $G = (V, E)$ in d dimensions, we therefore propose a two-step approach that determines positions $P \in \mathbb{R}^{n \times d}$ from graph-theoretic distances $\delta_{ij} = d_G(i, j)$, $i, j \in V$, as follows:

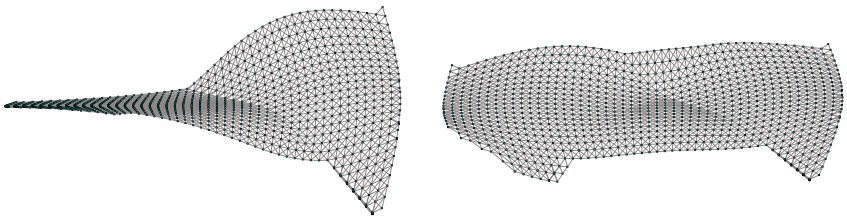

(a) 2D CMDS (b) 3D CMDS + WPCA

Fig. 7. Illustrating WPCA from 3D CMDS for `dwt1007` ($n = 1007$, $m = 4791$)

1. Construct an h-dimensional intermediate layout X using CMDS, where $d \leq h \ll n$ is chosen such that dissimilarities are represented sufficiently well.
2. Determine the final d-dimensional layout $P = X \cdot V$ using weighted PCA, where $V \in \mathbb{R}^{h \times d}$ is chosen such that total squared edge length is maximized.

Our approach thus exploits the best of both methods: CMDS constructs positions one coordinate at a time until the representation error is small, even if this requires more than d dimensions. PCA then determines a projection with the least degenerate edges.

In the subsequent sections we provide the details for both steps. Although there are several related methods, we believe that the approach advocated here is novel. There are at least three methods, though, that follow the same pattern of high-dimensional embedding with subsequent projection: HDE [19] uses graph-theoretic distances from selected vertices as high-dimensional coordinates and then applies (unweighted) PCA, so that dimensions are de-correlated but occlusion is not addressed. Similarly, GRIP [12] uses random linear projection of a higher-dimensional force-directed layout. In [20,21], user-controlled projection of high-dimensional CMDS drawings is proposed as an interaction technique.

4.1 High-Dimensional Layout

Since lower dimensions capture mostly the spread of a graph into different directions, more dimensions are needed to represent local details. But how many? Every output dimension added to CMDS is scaled by the square-root of the corresponding eigenvalue of B, so a dimension with a small eigenvalue does not change much anymore. There is, however, no proven criterion as to when to stop.

A common choice is to look for an eigengap, since data with an intrinsic dimensionality such as points from an h-dimensional manifold also yield a noticable gap between the h^{th} and $(h+1)^{th}$ positive eigenvalue. For graphs, however, it has also been suggested to use the entire positive part of the spectrum [20] of B.

We suggest an alternative based on marginal contribution. Let $\lambda_1 \geq \lambda_2, \ldots, \lambda_r$ be the largest positive eigenvalues of B, where r is an upper limit on the number of dimensions and chosen according to three criteria: the number of positive

eigenvalues, the number of pivots in approximate CMDS, and running time. Then we choose $d \leq h \leq r$ as the minimum index for which

$$\frac{\lambda_{h+1}}{\sum_{i=1}^{h} \lambda_i} < \varepsilon \tag{4}$$

for some minimum relative contribution of ε. Here, we let $\varepsilon = 0.05$.

Using PivotMDS [3] for approximate CMDS on a connected graph with n vertices and hence $m \in \Omega(n)$ edges, an h-dimensional embedding requires $\mathcal{O}(k(m+kn)+hk^3)$ time, where k is the number of pivots. Since $k = 150$ is usually more than enough, additional output dimensions therefore do not affect running time by much.

4.2 Final Projection

The first step resulted in $X \in \mathbb{R}^{n \times h}$. By linear projection with an orthonormal matrix $V \in \mathbb{R}^{h \times d}$ determined below we will obtain $P \in \mathbb{R}^{n \times d}$,

$$P = X \cdot V \ .$$

With $v^{(i)}$ we denote the i^{th} column of $V \in \mathbb{R}^{h \times d}$. A CMDS/PCA solution would correspond to V having first d columns of $I_h \in \mathbb{R}^{h \times h}$. Since we would also like to show some of the local structure otherwise hidden in the last $h - d$ dimensions, however, we use the following weighted variant of PCA.

Given a symmetric, non-negative weight matrix $W = (w_{ij}) \in \mathbb{R}^{n \times n}_{\geq 0}$, the *(weighted) Laplacian matrix* $L_W = (\ell_{ij}) \in \mathbb{R}^{n \times n}$ is defined by

$$\ell_{ij} = \begin{cases} \sum_{k \neq i} w_{ik} & \text{if } i = j \\ -w_{ij} & \text{otherwise .} \end{cases}$$

A layout P of orthonormal eigenvectors associated with the smallest (largest) eigenvalues of L_W minimize (maximize) the quadratic form

$$P^T L_W P = \sum_{i,j} w_{ij} \|p_i - p_j\|^2 \tag{5}$$

subject to $\|p^{(i)}\| = 1$ for $i = 1, \ldots, d$, and $p^{(i)} \perp p^{(j)}$ for $1 \leq i < j \leq d$. This is the basis of Laplacian spectral layout [18].

In our situation, positions are constrained to $P = XV$ for given X, so that $P^T L_W P = V^T X^T L_W X V$, and an optimal V is obtained by spectral decomposition of $X^T L_W X$, and thus weighted PCA (WPCA). In maximizing (5) by WPCA, we require $\|v^{(i)}\| = 1$ for $i = 1, \ldots, d$, and $v^{(i)} \perp v^{(j)}$ for $1 \leq i < j \leq d$, i.e., orthonormality of the direction vectors rather than the final positions.

Weights can be chosen for different purposes [25], but since we want the final $P \in \mathbb{R}^{n \times d}$ to display local graph structure, we set $W = A(G)$ to the adjacency matrix of the graph. According to (5), this maximizes the sum of

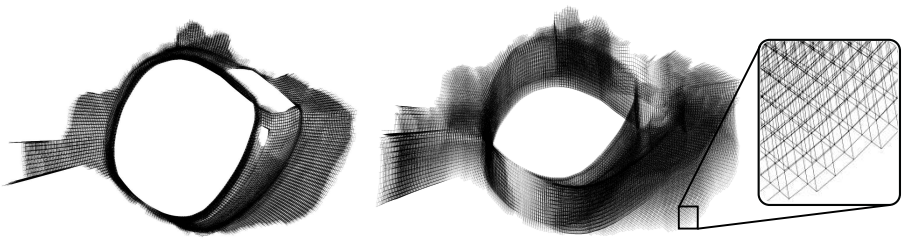

(a) 2D CMDS (b) 6D CMDS + WPCA, $\kappa = 750$

Fig. 8. WPCA drawing of graph `feOcean` ($n = 143437$, $m = 409593$)

squared edge lengths. Fig. 7(b) depicts WPCA result from a CMDS solution with h determined by (4). In certain cases, however, it is beneficial to symmetrically extend $W = A(G)$ by $\kappa \ll m$ edges chosen uniformly at random, in order to avoid close placement of some non-adjacent nodes, see Fig. 8.

In summary, we need to determine d eigenvectors associated with the largest eigenvalues of $X^T L_W X$, which is an $h \times h$ matrix constructed in $\mathcal{O}(h(m+hn))$, and then project $P = XV$ in $\mathcal{O}(nhd)$.

4.3 Relation to Choice of Origin

We conclude this section by showing that a d-dimensional CMDS solution from h-dimensional input centered on some vertex actually corresponds to a WPCA projection. We also provide an optimality criterion related to the choice of origin.

Lemma 1. *Given some input configuration $X \in \mathbb{R}^{n\times h}$, a CMDS solution $\widetilde{P} \in \mathbb{R}^{n\times d}$, $d \le h$, centered at some $k \in V$, corresponds to a WPCA solution $P \in \mathbb{R}^{n\times d}$ that maximizes*

$$\sum_{i\in\{1,\dots,n\},\ i\neq k} \|p_i - p_k\|^2 \ , \tag{6}$$

up to the position of the origin.

Proof. A d-dimensional CMDS projection from $S_k \cdot X \in \mathbb{R}^{n\times h}$ is obtained by $\widetilde{P} = S_k X \cdot Q$, with $Q \in \mathbb{R}^{h\times d}$ comprising orthonormal eigenvectors of $X^T(S_k^T S_k)X$ that correspond to its d largest eigenvalues. Note that $(S_k^T S_k) = L_W$, with L_W denoting a Laplacian that gives rise to (6) in the context of WPCA.

Since (W)PCA assumes a centered input X and yields a centered output P, the left multiplication by S_k in $\widetilde{P} = S_k X \cdot Q$ implies that $\widetilde{P}$ and P differ only in the position of the origin. □

5 Discussion

We have adapted classical multidimensional scaling (CMDS) for graph drawing in two ways: by transforming the input to produce focus+context layouts, and

by dividing it into a high-dimensional embedding with subsequent projection to avoid certain forms of degeneracies.

Combined with fast approximate CMDS, the first adaptation can be used interactively, and the second to produce improved layouts of very large graphs.

While CMDS has many advantages, several limitations remain. Despite its tendency to show symmetries very well, it fails in case of maximal symmetry. If large eigenvalues have higher multiplicity, it is not clear how to choose a unique and appropriate orthonormal basis in the associated invariant subspace. Other topics for future research include a reliable criterion to determine the intermediate layout dimensionality h, and the investigation of alternative projection weights that emphasize other features of a graph.

Acknowledgments. We gratefully acknowledge financial support from Deutsche Forschungsgemeinschaft (DFG) under grant GRK 1042.

References

1. Bavaud, F.: On the Schoenberg transformations in data analysis: Theory and illustrations. Journal of Classification 28(3), 297–314 (2011)
2. Borg, I., Groenen, P.: Modern Multidimensional Scaling: Theory and Applications. Springer (2005)
3. Brandes, U., Pich, C.: Eigensolver Methods for Progressive Multidimensional Scaling of Large Data. In: Kaufmann, M., Wagner, D. (eds.) GD 2006. LNCS, vol. 4372, pp. 42–53. Springer, Heidelberg (2007)
4. Brandes, U., Pich, C.: An Experimental Study on Distance-Based Graph Drawing. In: Tollis, I.G., Patrignani, M. (eds.) GD 2008. LNCS, vol. 5417, pp. 218–229. Springer, Heidelberg (2009)
5. Buja, A., Swayne, D.F., Littmann, M.L., Dean, N., Hofmann, H.: Xgvis: Interactive data visualization with mds. Journal of Computational and Graphical Statistics (2001)
6. Card, S.K., Mackinlay, J.D., Shneiderman, B. (eds.): Readings in Info. Vis.: Using Vision to Think. Morgan Kaufman Publishers (1999)
7. Civril, A., Magdon-Ismail, M., Bocek-Rivele, E.: SDE: Graph Drawing Using Spectral Distance Embedding. In: Healy, P., Nikolov, N.S. (eds.) GD 2005. LNCS, vol. 3843, pp. 512–513. Springer, Heidelberg (2006)
8. Çivril, A., Magdon-Ismail, M., Bocek-Rivele, E.: SSDE: Fast Graph Drawing Using Sampled Spectral Distance Embedding. In: Kaufmann, M., Wagner, D. (eds.) GD 2006. LNCS, vol. 4372, pp. 30–41. Springer, Heidelberg (2007)
9. Cox, T., Cox, M.: Multidimensional Scaling. CRC/Chapman and Hall (2001)
10. France, S.L., Carroll, J.D.: Two-way multidimensional scaling: A review. IEEE Trans. Sys., Man, and Cyber., Part C: Apps. and Reviews 41(5), 644–661 (2011)
11. Furnas, G.W.: Generalized fisheye views. In: Proc. ACM SIGCHI Conf. Human Factors in Comp. Sys., pp. 16–23. ACM Press (1986)
12. Gajer, P., Goodrich, M.T., Kobourov, S.G.: A Multi-dimensional Approach to Force-Directed Layouts of Large Graphs. In: Marks, J. (ed.) GD 2000. LNCS, vol. 1984, pp. 211–221. Springer, Heidelberg (2001)
13. Gansner, E., Koren, Y., North, S.: Topological fisheye views for visualizing large graphs. IEEE Trans. Vis. and Comp. Graph. 11(4), 457–468 (2005)

14. Gansner, E.R., Koren, Y., North, S.: Graph Drawing by Stress Majorization. In: Pach, J. (ed.) GD 2004. LNCS, vol. 3383, pp. 239–250. Springer, Heidelberg (2005)
15. Gower, J.C.: Some distance properties of latent root and vector methods used in multivariate analysis. Biometrika 53, 325–338 (1966)
16. Gower, J.C.: Euclidean distance geometry. Math. Scientist. 7, 1–14 (1982)
17. Gower, J.C.: Properties of Euclidean and non-Euclidean distance matrices. Linear Algebra and Its Applications 67, 81–97 (1985)
18. Hall, K.M.: An r-dimensional quadratic placement algorithm. Management Science 17, 219–229 (1970)
19. Harel, D., Koren, Y.: Graph Drawing by High-Dimensional Embedding. In: Goodrich, M.T., Kobourov, S.G. (eds.) GD 2002. LNCS, vol. 2528, pp. 207–219. Springer, Heidelberg (2002)
20. Hosobe, H.: A high-dimensional approach to interactive graph visualization. In: Proc. of ACM Symp. on Applied Comp., pp. 1253–1257. ACM (2004)
21. Hosobe, H.: An extended high-dimensional method for interactive graph drawing. In: Proc. of the Asia-Pac. Info. Vis., pp. 15–20. Austral. Comp. Soc. (2005)
22. Kaugars, K., Reinfelds, J., Brazma, A.: A Simple Algorithm for Drawing Large Graphs on Small Screens. In: Tamassia, R., Tollis, I.G. (eds.) GD 1994. LNCS, vol. 894, pp. 278–281. Springer, Heidelberg (1995)
23. Keahey, T.A., Robertson, E.L.: Techniques for non-linear magnification transformations. In: Proc. IEEE Symp. Info. Vis., pp. 38–46. IEEE Comp. Soc. (1996)
24. Koren, Y., Carmel, L.: Visualization of labeled data using linear transformations. In: Proc. IEEE Symp. Info. Vis., pp. 121–128. IEEE Comp. Soc. (2003)
25. Koren, Y., Carmel, L.: Robust linear dimensionality reduction. IEEE Trans. Vis. and Compr. Graph. 10(4), 459–470 (2004)
26. Kruskal, J.B., Seery, J.B.: Designing network diagrams. In: Proc. of the 1st Gen. Conf. on Soc. Graph., pp. 22–50 (1980)
27. Misue, K., Sugiyama, K.: Multi-viewpoint perspective display methods: Formulation and application to compound graphs. In: Proc. Conf. on HCI, pp. 834–838. Elsevier (1991)
28. Sarkar, M., Brown, M.H.: Graphical fisheye views of graphs. In: Proc. Conf. on HCI, pp. 83–91. ACM (1992)
29. de Silva, V., Tenenbaum, J.B.: Global versus local methods in nonlinear dimensionality reduction. In: Adv. Neur. Info. Process. Sys., vol. 15, pp. 705–712. MIT Press (2003)
30. Storey, M.D., David Fracchia, F., Mueller, H.A.: Customizing a fisheye view algorithm to preserve the mental map. Jour. Vis. Lang. Comp. 10(3), 245–267 (1999)
31. Torgerson, W.S.: Multidimensional scaling: I. Theory and method. Psychometrika 17(4), 401–419 (1952)
32. Tzeng, J., Lu, H.H.S., Li, W.H.: Multidimensional scaling for large genomic datasets. BMC Bioinformatics 9(1), 179–197 (2008)
33. Webb, A.R.: Statistical Pattern Recognition. John Wiley & Sons (2002)